

Digallane with Redox-Active Diimine Ligand: Dualism of Electron-Transfer Reactions

Igor L. Fedushkin,^{*,†,‡} Alexandra A. Skatova,[†] Vladimir A. Dodonov,[†] Valentina A. Chudakova,[†] Natalia L. Bazyakina,[†] Alexander V. Piskunov,^{†,‡} Serhiy V. Demeshko,[§] and Georgy K. Fukin^{†,‡}

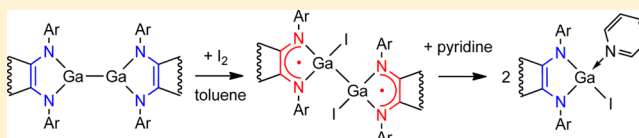
[†]G. A. Razuvaev Institute of Organometallic Chemistry of Russian Academy of Sciences, Tropinina 49, Nizhny Novgorod 603950, Russian Federation

[‡]Nizhny Novgorod State University, Prospect Gagarina 23, Nizhny Novgorod 603950, Russian Federation

[§]Institut für Anorganische Chemie, Georg-August-Universität, Tammannstrasse 4, Göttingen 37077, Germany

Supporting Information

ABSTRACT: The reactivity of digallane (dpp-Bian)Ga–Ga(dpp-Bian) (**1**), which consists of redox-active ligand 1,2-bis[(2,6-diisopropylphenyl)imino]acenaphthene (dpp-Bian), has been studied. The reaction of **1** with I₂ proceeds via one-electron oxidation of each of two dpp-Bian ligands to a radical-anionic state and affords complex (dpp-Bian)IGa–GaI(dpp-Bian) (**2**). Dissolution of complex **2** in pyridine (Py) gives monomeric compound (dpp-Bian)GaI(Py) (**3**) as a result of a solvent-induced intramolecular electron transfer from the metal–metal bond to the dpp-Bian ligands. Treatment of compound **3** with B(C₆F₅)₃ leads to removal of pyridine and restores compound **2**. The reaction of compound **1** with 3,6-di-*tert*-butyl-*ortho*-benzoquinone (3,6-Q) proceeds with oxidation of all the redox-active centers in **1** (the Ga–Ga bond and two dpp-Bian dianions) and results in mononuclear catecholate (dpp-Bian)Ga(Cat) (**4**) (Cat = [3,6-Q]²⁻). Treatment of **4** with AgBF₄ gives a mixture of [(dpp-Bian)₂Ag][BF₄] (**5**) and (dpp-Bian)GaF(Cat) (**6**), which both consist of neutral dpp-Bian ligands. The reduction of benzylideneacetone (BA) with **1** generates the BA radical-anions, which dimerize, affording (dpp-Bian)Ga–(BA–BA)–Ga(dpp-Bian) (**7**). In this case the Ga–Ga bond remains unchanged. Within 10 min at 95 °C in solution compound **7** undergoes transformation to paramagnetic complex (dpp-Bian)Ga(BA–BA) (**8**) and metal-free compound C₃₆H₄₀N₂ (**9**). The latter is a product of intramolecular addition of the C–H bond of one of the *i*Pr groups to the C=N bond in dpp-Bian. Diamagnetic compounds **3**, **5**, **6**, and **9** have been characterized by NMR spectroscopy, and paramagnetic complexes **2**, **4**, **7**, and **8** by ESR spectroscopy. Molecular structures of **2**–**7** and **9** have been established by single-crystal X-ray analysis.



INTRODUCTION

One of the modern concepts in the field of catalysis concerns the use of metal complexes of redox-active ligands for activation of organic molecules, thus allowing their further chemical transformation.¹ According to the concept, redox-active ligands should store and release electrons during catalytic processes as transition metal ions do in classical catalytic systems, e.g., Pd, Rh, and Ru.² However, all the catalysts of this new generation are still limited to the derivatives of transition metals, namely, Ir,³ Rh,⁴ Fe,⁵ Re,⁶ Zr,⁷ Ta,⁸ Ti,⁹ and Cu.¹⁰

Since 2003 we have been interested in the preparation of main-group metal complexes, which may emulate specific reactivity of coordination and organometallic compounds of transition metals. At the beginning we have found that the magnesium complex (dpp-Bian)Mg(thf)₃,¹¹ which contains the redox-active chelating ligand 1,2-bis[(2,6-diisopropylphenyl)imino]acenaphthene (dpp-Bian), is highly reactive toward some organic compounds.¹² In contrast to transition metals,¹³ in complexes of group 1, 2, 13, and 14 elements dpp-Bian may act as a radical-anionic (dpp-Bian) or dianionic ligand (dpp-Bian)^{11,14,15} and can undergo one-electron reduction or oxidation processes while still coordinated to the metal. This

feature of the dpp-Bian ligand in main-group metal complexes is correlated to the ability of transition metals to change their oxidation state within catalytic processes. However, realization of two-electron oxidative addition on the main-group metal complexes of dpp-Bian is difficult. For example, the dianion of dpp-Bian in the complex (dpp-Bian)Mg(thf)₃ can give up two electrons when reacting with oxidants. However, this leads to formation of neutral dpp-Bian, which, unfortunately, is not able to retain coordination to magnesium. In part this problem can be solved using metals that possess of two oxidation states differing in a unit of charge, e.g., a Sm²⁺/Sm³⁺ couple. But, the release of two electrons by complex (dpp-Bian)²⁻Sm²⁺(dme)₃ in the course of its reactions with oxidizing reagents occurs in fact as two independent one-electron processes. Thus, the reaction of (dpp-Bian)²⁻Sm²⁺(dme)₃ with 1 molar equiv of Ph(Br)CHCH(Br)Ph affords complex [(dpp-Bian)⁻Sm³⁺Br₂(dme)₃]₂, in which both redox-active centers are oxidized in comparison with the starting complex. On the other hand the reaction of (dpp-Bian)²⁻Sm²⁺(dme)₃ with 0.5

Received: February 1, 2014

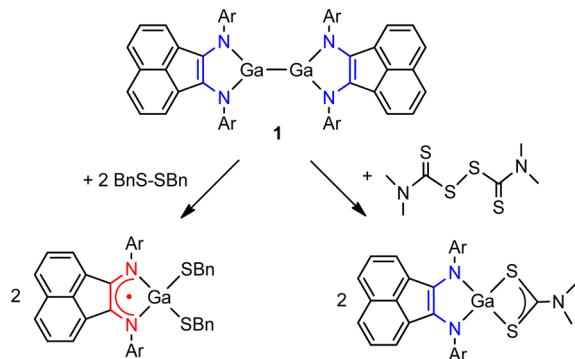
Published: May 8, 2014



molar equiv of $\text{Ph}(\text{Br})\text{CHCH}(\text{Br})\text{Ph}$ produces stable compound $(\text{dpp-Bian})^{2-}\text{Sm}^{3+}\text{Br}(\text{dme})_3$, in which the oxidation state of the only metal center is altered.¹⁶

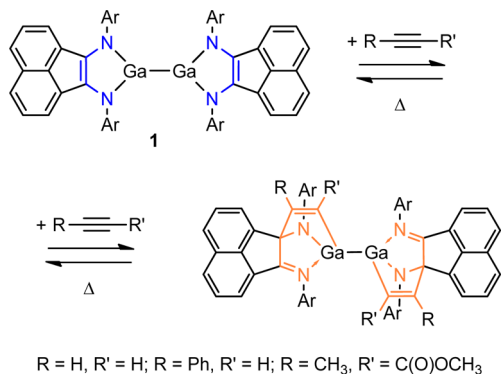
A remarkable reactivity has been observed for $(\text{dpp-Bian})\text{Ga-Ga}(\text{dpp-Bian})$ (**1**).¹⁷ Since a formal oxidation state of the metal atoms in **1** is +2, this compound behaves to some extent similar to complex $(\text{dpp-Bian})^{2-}\text{Sm}^{2+}(\text{dme})_3$. The reaction of **1** with 2 molar equiv of $\text{PhCH}_2\text{S-SCH}_2\text{Ph}$ produces $(\text{dpp-Bian})^-\text{Ga}^{3+}(\text{SCH}_2\text{Ph})_2$, while the reaction of **1** with 1 molar equiv of $\text{Me}_2\text{N}(\text{S})\text{CS-SC}(\text{S})\text{NMe}_2$ gives $(\text{dpp-Bian})^{2-}\text{Ga}^{3+}(\text{S}_2\text{CNMe}_2)$ (Scheme 1).¹⁸ In the reactions of

Scheme 1. Reactivity of Compound **1** toward Disulfides



$(\text{dpp-Bian})\text{Ga-Ga}(\text{dpp-Bian})$ (**1**) with alkynes no electron transfer from compound **1** to the substrate takes place, but the ligand exhibits a marvelous lability with the ligand being directly involved in bonding of the substrate (Scheme 2).¹⁹ Amazingly,

Scheme 2. Reactivity of compound **1** towards alkynes



the addition of alkynes by complex **1** is reversible. The ability of complex **1** to coordinate phenylacetylene allows its catalytic functionalization including hydroamination and hydroarylation with anilines.^{19b} It is worth mentioning that catalytic activity of compound **1** in hydroamination of $\text{PhC}\equiv\text{CH}$ with aromatic amines is comparable with the activity of transition metal-based systems.²⁰ The extensive study on reactions of group 13 metal-metal bond-containing compounds is reported.²¹

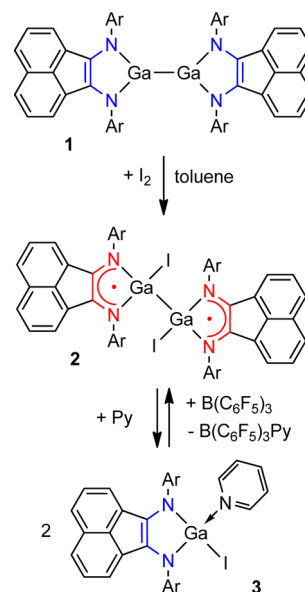
Here we report a new type of reactivity of compound **1**. We demonstrate that in the reactions with some substrates oxidation of the dianionic dpp-Bian ligands in **1** can take place before oxidation of the metal-metal bond. In fact, we were able to perform concerted two-electron oxidative addition to the Ga-Ga center in the complex $(\text{dpp-Bian})\text{Ga-Ga}(\text{dpp-Bian})$. In this process the empty orbitals for the binding of the

substrate by complex **1** are recruited from the metal, while the electrons are provided by the ligand.

RESULTS AND DISCUSSION

Reactions of Compound 1 with Oxidizing Reagents. Formation and Spectroscopic Characterization of $(\text{dpp-Bian})\text{IGa-GaI}(\text{dpp-Bian})$ (2**), $(\text{dpp-Bian})\text{GaI}(\text{Py})$ (**3**), $(\text{dpp-Bian})\text{Ga}(\text{Cat})$ (**4**), $[(\text{dpp-Bian})_2\text{Ag}][\text{BF}_4]$ (**5**), $(\text{dpp-Bian})\text{GaF}(\text{Cat})$ (**6**), $(\text{dpp-Bian})\text{Ga}(\text{BA-BA})\text{Ga}(\text{dpp-Bian})$ (**7**), $(\text{dpp-Bian})\text{Ga}(\text{BA-BA})$ (**8**), and $\text{C}_{36}\text{H}_{40}\text{N}_2$ (**9**).** Treatment of compound **1** with 1 molar equiv of I_2 in toluene results in an immediate color change from deep blue, which is typical for dpp-Bian^{2-} , to red, which is indicative for the formation of dpp-Bian^- . The product $(\text{dpp-Bian})\text{IGa-GaI}(\text{dpp-Bian})$ (**2**) is poorly soluble in toluene and precipitates from the reaction mixture as a red crystalline powder (Scheme 3).

Scheme 3. Syntheses of Compounds **2** and **3**

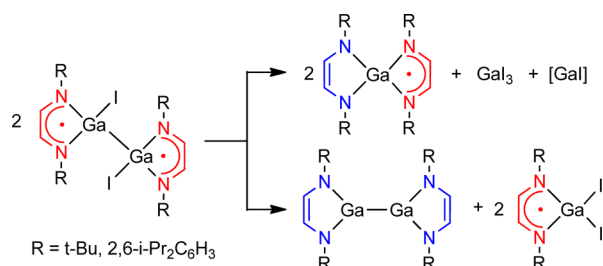


Crystallization of the crude product from hot 1,2-dimethoxyethane resulted in compound **2** (47%) as deep red, prismatic crystals. Addition of 2 molar equiv of I_2 to the toluene solution of **1** results in a clear red solution, from which compound $(\text{dpp-Bian})\text{GaI}_2$ was isolated. The latter has been previously obtained by reacting dpp-Bian with "GaI".²² Dissolution of complex **2** in pyridine resulted in a color change from red to deep blue. Crystallization from toluene gives $(\text{dpp-Bian})\text{GaI}(\text{Py})$ (**3**) (Scheme 3) as deep blue, nearly black crystals in 63% yield. It is worth mentioning that compound **3** is formed in the course of a solvent-induced intramolecular electron transfer from the Ga-Ga bond to two dpp-Bian ligands in complex **2**. One may expect that removing pyridine from complex **3** should restore binuclear compound **2**. In fact we have found that addition of 1 molar equiv of $\text{B}(\text{C}_6\text{F}_5)_3$ to a solution of complex **3** in toluene results in the formation of dinuclear compound **2**, isolated in 28% yield after crystallization from 1,2-dimethoxyethane. This process is a sort of redox-isomerism that is well established in 3d-metal complexes²³ and recently also in f-element series, e.g., ytterbium complexes of the dpp-Bian ligand, $[(\text{dpp-Bian})\text{YbX}(\text{dme})]_2$ ($\text{X} = \text{Cl},^{24a} \text{Br}^{24b}$). However, in the main-group metal complexes such a phenomenon is difficult to realize because of the lack of existence of at least two

stable oxidation states and facile shuttling between them in s- and p-metal series.

Despite the presence of the ligands bearing an unpaired electron compound **2** does not reveal well resolved ESR signal: only a broad signal could be detected in the solid state as well as in solution (toluene or 2-Me-THF) in a temperature range 360–120 K. This observation allows making two conclusions. First, compound **2** does not disproportionate in solution into mononuclear radical species as in the case of related gallium complexes²⁵ (Scheme 4). Second, unpaired electrons of dpp-Bian radicals are antiferromagnetically coupled.

Scheme 4. Two Pathways of Disproportionation of Diazadiene Digallanes



The existence of an antiferromagnetic exchange between unpaired electrons in the molecule of complex **2** has been further confirmed by the measurements of the magnetic susceptibility of the crystalline sample. A temperature dependence of the magnetic moment of compound **2** is shown in Figure 1.

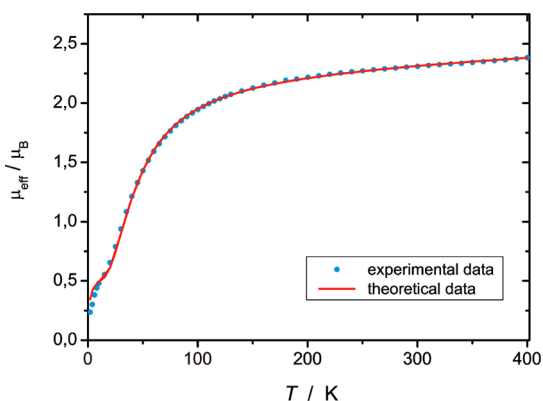


Figure 1. Temperature dependence of the magnetic moment of compound **2**. The solid line shows the best fit curve (see text).

At ambient temperature the magnetic moment of compound **2** is close to the value calculated for two noninteracting ligand-localized unpaired electrons ($\mu_{\text{eff}} = [(1.73)^2 + (1.73)^2]^{1/2} = 2.45 \mu_{\text{B}}$). Lowering the temperature from 400 K to 150 K results in a monotonic decrease of the magnetic moment. Below 150 K the value of μ_{eff} starts to decrease more rapidly, and at 2 K the sample behaves nearly as diamagnetic. The exchange coupling constant between spin carriers in **2** was determined by using a fitting procedure to the Heisenberg–Dirac–van-Vleck (HDvV) spin Hamiltonian for isotropic exchange coupling and Zeeman splitting, eq 1.

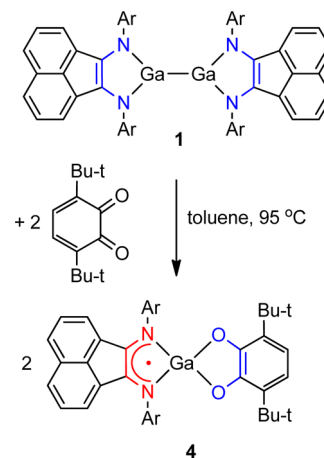
$$\hat{H} = -2J\hat{S}_1 \cdot \hat{S}_2 + g\mu_{\text{B}}(\vec{S}_1 + \vec{S}_2) \cdot \vec{B} \quad (1)$$

Temperature-independent paramagnetism (TIP) and a Curie-behaved paramagnetic impurity (PI) with spin $S = 1/2$ were included according to $\chi_{\text{calc}} = (1 - \text{PI})\chi + \text{PI}\chi_{\text{mono}} + \text{TIP}$. The obtained fit parameters are $J = -38 \text{ cm}^{-1}$, $g = 1.92$, $\text{PI} = 9.5\%$, and $\text{TIP} = 2.4 \times 10^{-4} \text{ cm}^3 \text{ mol}^{-1}$. The relatively high coupling constant indicates an effective mediation of the digallane bridge in the exchange interaction. Since an inspection of the crystal packing in **2** (*vide infra*) has revealed a π stacking between the naphthalene rings of the neighboring molecules, an intermolecular antiferromagnetic exchange probably takes place. This intermolecular interaction provides for the formation of indefinite 1D polymeric chains in the crystals of compound **2** and makes complex **2** poorly soluble. An example of an extreme form of such coupling resulted in a C–C bond, reported recently for related indium diimine complexes.²⁶

Compound **3** is diamagnetic, its ^1H NMR spectrum in C_6D_6 reveals an expected signal set for the dpp-Bian dianion. In free dpp-Bian as well as in the coordinated dpp-Bian ligand a rotation of the Ph rings ($\text{N}-\text{C}_{\text{ipso}}$) as well as the *i*Pr substituents ($\text{C}(\text{H})-\text{C}_{\text{ipso}}$) is not possible due to steric reasons. In contrast to free dpp-Bian, which consists of two mirror planes, only one plane of symmetry (defined with atoms I, Ga, and N) is present in the molecule of complex **3**. Therefore, its ^1H NMR spectrum consists of four doublets of methyl groups (δ 1.57, 1.23, 1.13, 0.33 ppm) and two septets of the methine protons (δ 3.95, 3.27 ppm).

In contrast to the reaction with iodine, the oxidation of complex **1** with 3,6-di-*tert*-butyl-*ortho*-benzoquinone (3,6-Q) proceeds only at elevated temperatures. At 95 °C the reaction is accompanied by a color change from deep blue to green within 1 h. At the molar ratio 1 to 2 (complex **1** to 3,6-Q) catecholate (dpp-Bian)Ga(Cat) (**4**) (Cat = $[\text{3,6-Q}]^{2-}$) was isolated in 80% yield (Scheme 5). Complex **4** resulted from oxidation of all the

Scheme 5. Oxidation of Compound 1 with 3,6-Di-*tert*-butyl-*ortho*-benzoquinone (3,6-Q)



redox-active centers in **1**: the Ga–Ga bond and two dpp-Bian dianions. Due to the presence of the dpp-Bian radical-anion, complex **4** reveals a well-resolved ESR signal (Figure 2). The hyperfine structure of the signal is caused by the coupling of an unpaired electron to two pairs of protons (99.98%, $I = 1/2$, $\mu_{\text{N}} = 2.7928$),²⁵ to two equivalent ^{14}N nuclei (99.63%, $I = 1$, $\mu_{\text{N}} = 0.4037$),²⁷ and to gallium magnetic isotopes ^{69}Ga (60.11%, $I = 3/2$, $\mu_{\text{N}} = 1.8507$) and ^{71}Ga (39.89%, $I = 3/2$, $\mu_{\text{N}} = 2.56227$).²⁵ The ESR spectroscopy unequivocally indicates the presence in

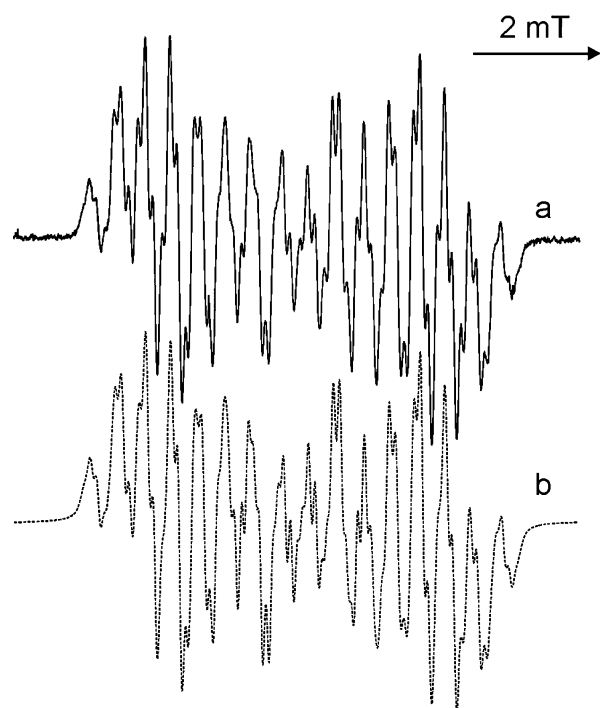


Figure 2. ESR spectrum of **4** (toluene, 293 K): (a) experimental; (b) simulated ($a_i(2\ ^{14}\text{N}) = 0.427\ \text{mT}$, $a_i(^{69}\text{Ga}) = 1.420\ \text{mT}$, $a_i(^{71}\text{Ga}) = 1.805\ \text{mT}$, $a_i(2\ ^1\text{H}) = 0.107\ \text{mT}$, $a_i(2\ ^1\text{H}) = 0.115\ \text{mT}$, $g = 2.0025$).

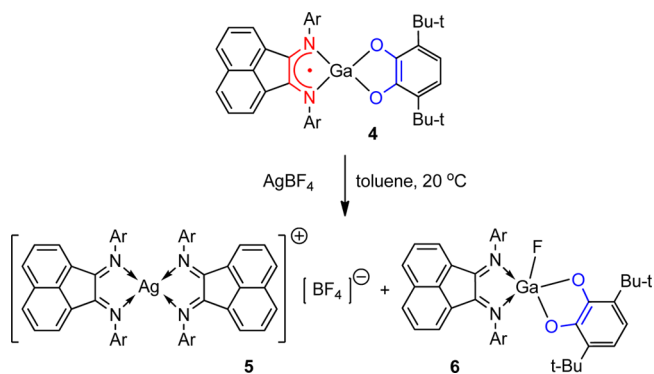
complex **4** of a radical-anion of the dpp-Bian. The catecholate nature of the quinone ligand in compound **4** is supported by its IR spectrum; the C–O stretching vibrations of neutral 3,6-BQ (1680 and $1640\ \text{cm}^{-1}$)²⁸ as well as its semiquinonic form (1485 and $1450\ \text{cm}^{-1}$)²⁶ are absent.

Looking for another example of oxidative addition to the Ga–Ga center in compound **1**, we carried out the reaction between **1** and acenaphthenequinone (AQ). Despite a more negative reduction potential of AQ compared to 3,6-Q, the reaction between **1** and AQ proceeds easily and results in the desired product. Detailed characterization of this product will be published elsewhere together with other related complexes.

In order to prepare a gallium complex containing two different radical-anionic ligands, namely, dpp-Bian and 3,6-SQ, we have studied oxidation of the 3,6-Cat ligand in complex **4** with AgBF_4 . To the best of our knowledge heteroligand biradicals have not been reported so far. The reaction between **4** and AgBF_4 proceeds at ambient temperature. One of the products of this reaction, $[(\text{dpp-Bian})_2\text{Ag}][\text{BF}_4]$ (**5**), starts to crystallize as orange crystals from the reaction mixture when evaporation of the solvent begins. Separation of crude product **5** and continued evaporation of the solvent from the mother liquor afforded deep green crystals of a second product, (dpp-Bian)GaF(Cat) (**6**) (Scheme 6). Both compounds **5** and **6** consist of neutral dpp-Bian ligands. Thus, oxidation of the dpp-Bian radical-anion to neutral dpp-Bian takes place before oxidation of catecholate ligand to its semiquinonic state. It should be also noted that product **6** consists of fluorine as the anionic ligand, not the BF_4 anion. Compound **5** can be prepared also in good yield just by reacting dpp-Bian with AgBF_4 .

Both compounds **5** and **6** are diamagnetic; they have been characterized by IR and ^1H NMR spectroscopy. Similar to complex **3**, in compound **6** there is no mirror plane that

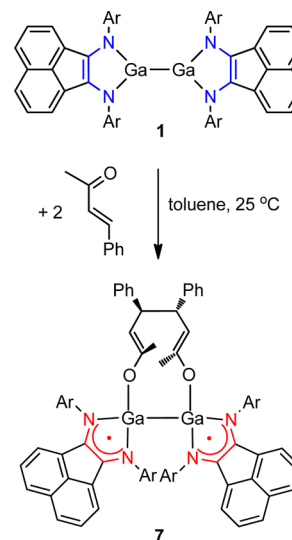
Scheme 6. Oxidation of Complex **4** with AgBF_4



coincides with the diimine plane. Therefore, the ^1H NMR spectrum of compound **6** consists of two septets (δ 3.66 and 2.64 ppm) and four doublets (δ 1.47, 1.18, 1.0 (overlap with *t*Bu signal), and 0.69 ppm).

Benzylideneacetone (BA) was chosen as a substrate for investigation of the reactivity of complex **1** because several reaction pathways may be expected. First, the reaction between **1** and BA can proceed as a 2+4 cycloaddition similar to that observed in the reactions of complex **1** with alkynes (Scheme 2). Such 2+4 cycloaddition of vinylacetone to aluminum complex (dpp-Bian)AlEt(Et₂O) has been recently observed.²⁹ Second, one may expect formation of ketyl radicals under electron transfer from complex **1** to BA. In this case the electrons can be provided either by the ligand or by the metal–metal bond. The BA ketyl radicals, in turn, may further dimerize to give a gallium pinacolate. In fact it has been found that reaction between compound **1** and BA in toluene easily proceeds at room temperature. Within a few minutes after mixing the reagents the toluene solution turned from deep blue to red-brown, thus indicating the formation of dpp-Bian radical-anionic species. Crystallization from the reaction mixture afforded dark brown crystals of compound (dpp-Bian)Ga–(BA–BA)–Ga(dpp-Bian) (**7**) in 26% yield (Scheme 7). Investigation of compound **7** by spectroscopic and crystallographic methods has shown that the compound consists of two radical-anionic dpp-Bian ligands, a gallium–gallium bond, and a

Scheme 7. Oxidation of Complex **1** with Benzylideneacetone



4,5-diphenylocta-2,6-diene-2,7-diolate fragment. The latter is formed in the course of dimerization of two BA radical-anions. Surprisingly, dimerization of two BA radical-anions occurred not at the α position to the oxygen atom but at the γ position. We believe that dimerization at the α position would not be optimal because of the stronger tensions in the six-membered metallacycle compared to the 10-membered metallacycle, which is observed in fact in the product 7. On the other hand in this case radical stability considerations also may play a role. Thus, stabilization of the putative radical at the γ -position to the oxygen atom may be provided by both phenylic and olefinic substituents. Compound 7 is paramagnetic due to the presence of two dpp-Bian radical-anions. However, no ESR signal could be observed in solution at ambient temperature. Only at 150 K in a toluene matrix does compound 7 give rise to an ESR signal, which clearly indicates the presence of the biradical species.

The distance between centers of localization of unpaired electrons in molecule 7 has been estimated using zero field splitting parameters ($|D| = 10$ mT, $|E| = 0.8$ mT). The calculated value is 6.52 Å. For comparison, according to the X-ray data, the distance between the middle points of the bonds C(1)–C(2) and C(1a)–C(2a) is 7.15 Å, whereas the distance between the geometrical centers defined with atoms N(1)–C(1)–C(2)–N(2) and N(1a)–C(1a)–C(2a)–N(2a) is 6.03 Å. A half-field ESR signal, which corresponds to a forbidden transition ($\Delta m_s = 2$), has also been observed (inset in Figure 3). Although this signal is broadened, its hyperfine structure

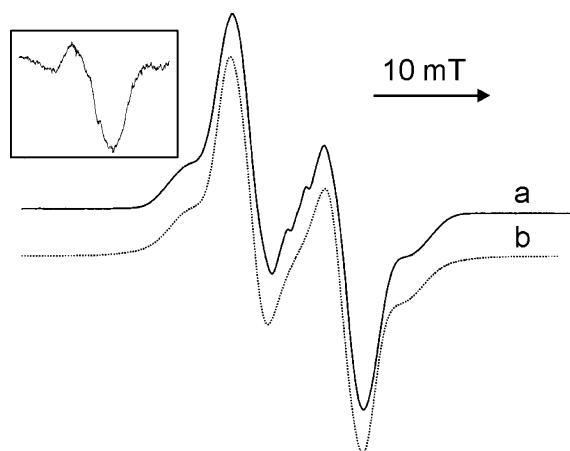


Figure 3. ESR signal of 7 (toluene, 150 K): (a) experimental; (b) simulated.

(septet) can be distinguished. This structure is caused by the presence in the molecule of 7 of two atoms of Ga, whose isotopes (^{69}Ga and ^{71}Ga) possess nuclear spin $I_N = 3/2$.

In solution complex 7 is unstable. Heating a toluene solution of complex 7 at 95 °C for 10 min gives rise to a well-resolved ESR signal (Figure 4), whose parameters allow suggesting the formation of mononuclear gallium complex (dpp-Bian)Ga-(BA-BA) (8) (Scheme 8).

Workup of the reaction mixture allows isolation of compound 9 in the form of yellow (Et_2O) or red crystals (hexane). Compound 9 represents a tautomeric form of dpp-Bian. It is formed in the course of the intramolecular addition of the C–H bond of one of the *i*Pr groups to the C=N bond in dpp-Bian. The hyperfine structure of the ESR signal of complex 8 is caused by the coupling of the unpaired electron to

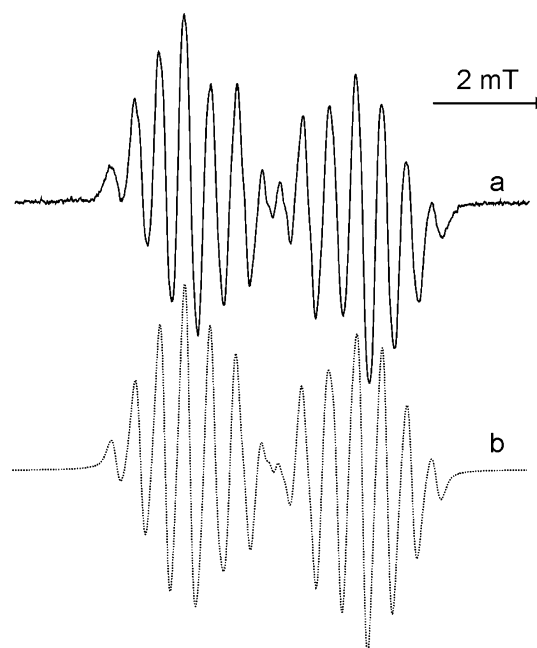
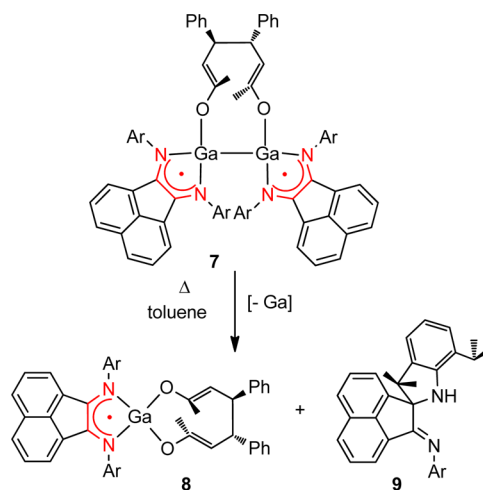


Figure 4. ESR signal of 8 (toluene, 297 K): (a) experimental ($a_1(2^{14}\text{N}) = 0.48$ mT, $a_1(^{69}\text{Ga}) = 1.125$ mT, $a_1(^{71}\text{Ga}) = 1.430$ mT, $g_i = 2.0026$); (b) simulated.

Scheme 8. Thermal Decomposition of 7 and Formation of Compounds 8 and 9



two equivalent ^{14}N nuclei and magnetic isotopes of gallium ^{69}Ga and ^{71}Ga .

Diamagnetic compound 9 has been characterized by IR and ^1H NMR spectroscopy. In contrast to dpp-Bian, which possesses two mirror planes, the molecule of compound 9 is asymmetric. Moreover, one of the carbon atoms of the newly formed C–C bond in compound 9 is chiral. The asymmetry of molecule 9 causes nonequivalence of all the carbon atoms as well as of all protons except the protons in the CH_3 groups.

Molecular Structures of 2–7 and 9. The molecular structures of compounds 2, 3, 4, 5, 6, 7, and 9 were determined by single-crystal X-ray diffraction and are depicted in Figures 5, 7, 8, 9, 10, 11, 12, correspondingly. The packing of molecules in the crystal of compound 2 is shown in Figure 6. The crystal data collections and structure refinement details are listed in Table 1.

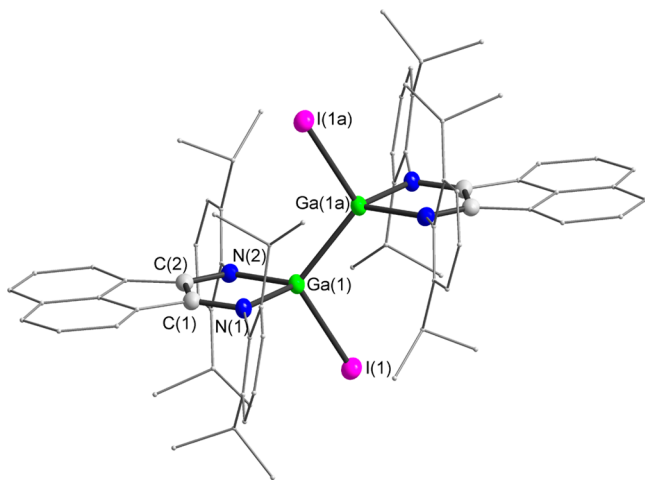


Figure 5. Molecular structure of **2**. Thermal ellipsoids are drawn at the 50% probability level. Hydrogen atoms are omitted. Selected bond lengths (Å) and angles (deg): Ga(1)–N(1) 1.997(2), Ga(1)–N(2) 1.999(2), Ga(1)–Ga(1a) 2.4655(5), Ga(1)–I(1) 2.5910(3), N(1)–C(1) 1.352(3), N(2)–C(2) 1.338(3), C(1)–C(2) 1.425(3), N(1)–Ga(1)–N(2) 84.95(8), N(1)–Ga(1)–Ga(1a) 119.38(6), N(2)–Ga(1)–Ga(1a) 120.14(6), N(1)–Ga(1)–I(1) 109.55(6), N(2)–Ga(1)–I(1) 109.48(6), Ga(1a)–Ga(1)–I(1) 110.781(17), C(1)–N(1)–Ga(1) 108.83(15), C(2)–N(2)–Ga(1) 109.40(16).

The molecule of compound **2** (Figure 5) is situated on the crystallographic inversion center, which is located at the middle of the gallium–gallium bond. Coordination tetrahedrons of both metal atoms are slightly distorted.

The acenaphthene-1,2-diimine planes are parallel to each other, with gallium atoms lying almost perfectly within the planes, estimated with atoms N(1)–C(1)–C(2)–N(2) and their symmetry equivalent counterparts. The Ga–Ga distance in compound **2** (2.4655(5) Å) corresponds to a covalent metal–metal bond. This distance is remarkably longer than that in complex **1** (2.3598(3) Å),³⁰ but it matches well the Ga–Ga distances in (*t*Bu-dad)IGa–GaI(*t*Bu-dad) (2.4232(7) Å)^{31a} and

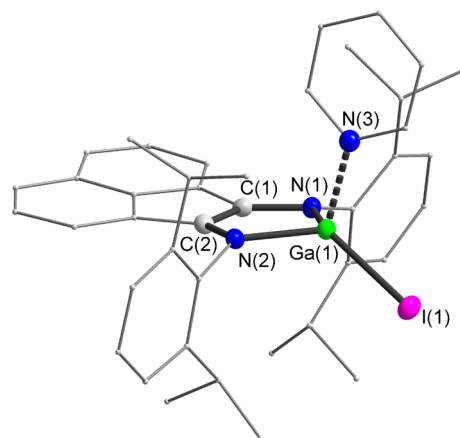


Figure 7. Molecular structure of **3**. Thermal ellipsoids are drawn at the 50% probability level. Hydrogen atoms are omitted. Selected bond lengths (Å) and angles (deg): Ga(1)–N(1) 1.906(2), Ga(1)–N(2) 1.887(2), Ga(1)–N(3) 2.042(2), Ga(1)–I(1) 2.4931(3), N(1)–C(1) 1.404(3), N(2)–C(2) 1.400(3), C(1)–C(2) 1.376(3), N(2)–Ga(1)–N(1) 92.03(8), N(2)–Ga(1)–N(3) 103.85(8), N(1)–Ga(1)–N(3) 104.01(8), N(2)–Ga(1)–I(1) 121.91(6), N(1)–Ga(1)–I(1) 128.29(6), N(3)–Ga(1)–I(1) 103.76(6).

(Ar-dad)IGa–GaI(Ar-dad) (2.5755(16) Å).^{31b} The equality of the Ga–N bonds in **2** (1.997(2) and 1.999(2) Å) indicates an effective delocalization of the electron density within the diimine fragment. In the crystal molecules of compound **2** are arranged in such a way that the acenaphthene rings are lying in planes that are entirely parallel to each other (Figure 6). The shortest distance between these planes is 3.40 Å. This value is close to the distance between the layers in graphite (3.35 Å).³² It is worth noting that earlier we have observed the formation of infinite 1D quasi-polymeric structures through the intermolecular π interaction between the ligands in the crystals of samarium and europium 2,2'-bipyridyl complexes Ln(bipy)₄ (Ln = Sm, Eu).³³ The distances between the planes of the 2,2'-bipyridyl ligands in these lanthanide complexes (Sm, 3.25 Å;

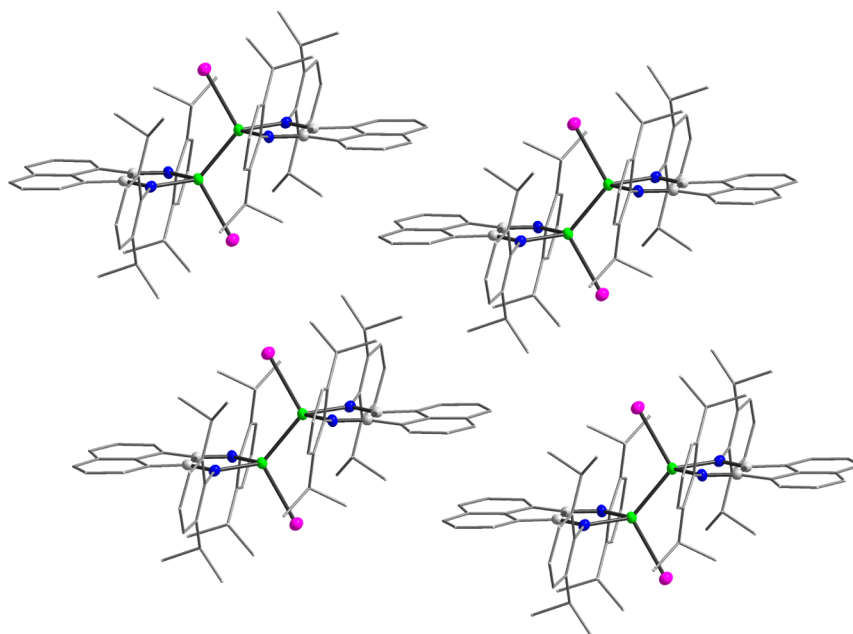


Figure 6. Crystal packing of compound **2**. The lattice DME molecules are omitted for clarity.

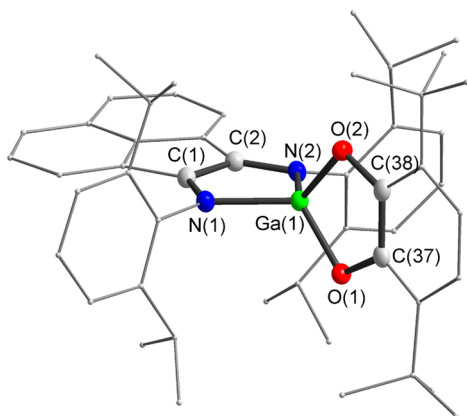


Figure 8. Molecular structure of **4**. Thermal ellipsoids are drawn at the 50% probability level. Hydrogen atoms are omitted. Selected bond lengths (Å) and angles (deg): Ga(1)–O(1) 1.8255(13), Ga(1)–O(2) 1.8269(13), Ga(1)–N(1) 1.9432(13), Ga(1)–N(2) 1.9335(16), O(1)–C(37) 1.380(2), O(2)–C(38) 1.372(2), C(37)–C(38) 1.414(3), N(1)–C(1) 1.336(2), N(2)–C(2) 1.343(2), C(1)–C(2) 1.431(2), O(1)–Ga(1)–O(2) 92.16(6), N(2)–Ga(1)–N(1) 87.54(6), O(1)–Ga(1)–N(2) 124.15(6), O(1)–Ga(1)–N(1) 118.24(6).

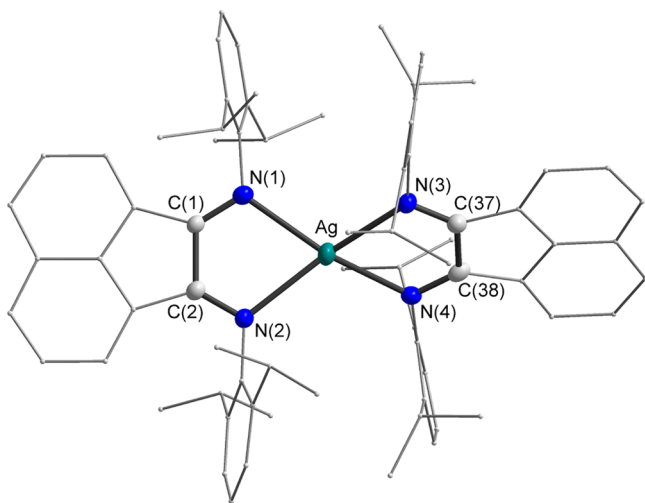


Figure 9. Molecular structure of the cation [(dpp-Bian)₂Ag]⁺ in **5**. Thermal ellipsoids are drawn at the 50% probability level. Hydrogen atoms are omitted. Selected bond lengths (Å) and angles (deg): Ag(1)–N(1) 2.334(3), Ag(1)–N(2) 2.374(3), Ag(1)–N(3) 2.378(3), Ag(1)–N(4) 2.311(3), N(1)–C(1) 1.260(4), N(2)–C(2) 1.271(4), C(1)–C(2) 1.528(4), N(3)–C(37) 1.281(4), N(4)–C(38) 1.276(4), C(37)–C(38) 1.529(5), N(1)–Ag(1)–N(2) 73.40(9).

Eu, 3.31 Å) are even shorter than interlayer distances in graphite. Accordingly, compounds are absolutely insoluble in organic media. We believe that intermolecular interaction in compound **2** is rather strong and responsible for the low solubility of the compound. Also, this interaction may provide an opportunity for the unpaired electrons to couple antiferromagnetically.

Compound **3** is a mononuclear four-coordinate complex (Figure 7). Due to the stronger interaction between Ga and the dpp-Bian dianion, the Ga–N bonds (Ga(1)–N(1) 1.906(2) and Ga(1)–N(2) 1.887(2) Å) in complex **3** are ca. 0.1 Å shorter than corresponding bonds in compound **2**, which consists of a dpp-Bian radical-anion. The Ga–I bond (2.4931(3) Å) in **3** is also remarkably shorter than the Ga–I

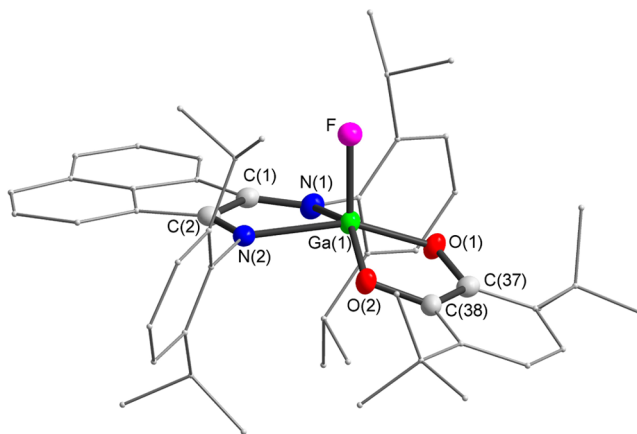


Figure 10. Molecular structure of **6**. Thermal ellipsoids are drawn at the 50% probability level. Hydrogen atoms are omitted. Selected bond lengths (Å) and angles (deg): Ga(1)–F(1) 1.795(7), Ga(1)–O(1) 1.859(0), Ga(1)–O(2) 1.854(8), Ga(1)–N(1) 2.087(7), Ga(1)–N(2) 2.120(1), N(1)–C(1) 1.278(2), N(2)–C(2) 1.284(2), C(1)–C(2) 1.517(2), O(1)–C(37) 1.355(2), O(2)–C(38) 1.361(2), C(37)–C(38) 1.418(2), F(1)–Ga(1)–O(2) 112.80(5), F(1)–Ga(1)–O(1) 110.09(5), F(1)–Ga(1)–N(1) 96.18(5), O(2)–Ga(1)–N(1) 149.33(6), O(2)–Ga(1)–O(1) 88.72(5), N(1)–Ga(1)–N(2) 78.98(6).

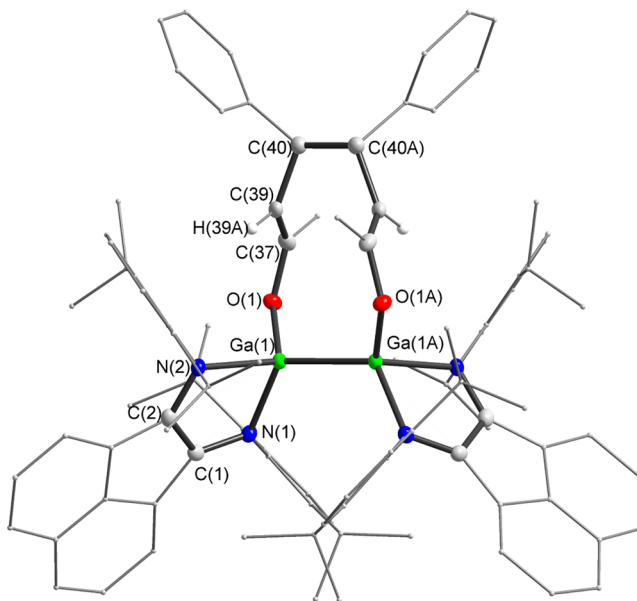


Figure 11. Molecular structure of **7**. Thermal ellipsoids are drawn at the 50% probability level. Hydrogen atoms are omitted. Selected bond lengths (Å) and angles (deg): Ga(1)–N(1) 2.0075(12), Ga(1)–N(2) 2.0258(12), Ga(1)–O(1) 1.8456(10), Ga(1)–Ga(1A) 2.4871(3), O(1)–C(37) 1.3646(18), N(1)–C(1) 1.3369(19), N(2)–C(2) 1.3370(19), C(1)–C(2) 1.441(2), C(37)–C(39) 1.331(2), C(39)–C(40) 1.508(2), C(40)–C(40A) 1.594(3), O(1)–Ga(1)–N(1) 98.91(5), O(1)–Ga(1)–N(2) 108.26(5), N(1)–Ga(1)–N(2) 84.30(5), O(1)–Ga(1)–Ga(1A) 117.11(3), N(1)–Ga(1)–Ga(1A) 123.77(4), N(2)–Ga(1)–Ga(1A) 118.83(4), C(37)–O(1)–Ga(1) 125.01(9).

bond in **2** (2.5910(3) Å). Probably, a shortening of the Ga–I distance in **3** compared to that distance in **2** is caused by a higher formal oxidation state of the gallium atom in complex **3** (+3) compared to compound **2** (+2).

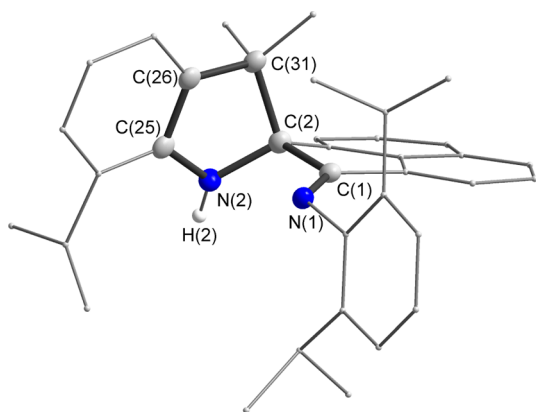


Figure 12. Molecular structure of **9**. Thermal ellipsoids are drawn at the 50% probability level. Hydrogen atoms are omitted. Selected bond lengths (Å) and angles (deg): N(1)–C(1) 1.2731(13), C(1)–C(2) 1.5671(14), C(2)–N(2) 1.4704(13), C(2)–C(31) 1.5863(14), N(2)–C(25) 1.4153(13), C(26)–C(31) 1.5203(14), N(1)–C(1)–C(2) 120.43(9), N(2)–C(2)–C(1) 112.89(8), N(2)–C(2)–C(31) 101.57(8), C(1)–C(2)–C(31) 111.07(8), C(25)–N(2)–C(2) 106.83(8).

Compound **4** is a mononuclear four-coordinate complex (Figure 8), which consists of two different redox-active ligands. The Ga–N and Ga–O distances are very close in the pairs. The Ga–N distances (1.9432(13) and 1.9335(16) Å) are ca. 0.6 Å shorter than corresponding distances in compound **2**, which consists of a radical-anionic dpp-Bian ligand. On the other hand, the Ga–O bonds in **4** are ca. 0.5 Å longer compared with those bonds in compound **3**. One can expect the existence of two redox isomers of compound **4**: (dpp-Bian)[−]Ga(3,6-Q)^{−2} or (dpp-Bian)^{−2}Ga(3,6-Q). To make the decision whether the dpp-Bian ligand in **4** acts as a radical-anion or dianion, an inspection of the bond distances within the diimine section is useful.

Thus, the C–N distances within the metallacycle in complex **4** (1.336(2) and 1.343(2) Å) are very close to those in compound **2** (1.352(3) and 1.338(3) Å), but remarkably shorter than in compound **3** (1.404(3) and 1.400(3) Å). Hence, the present structural data are in agreement with spectroscopic data (*vide supra*), which indicate the presence of the dpp-Bian radical-anion in compound **4**. Accordingly, 3,6-Q is present in **4** as a catecholate. For comparison, in neutral 3,6-Q the C=O distances are 1.207(2) and 1.214(2) Å.³⁴ The dihedral angle between the planes of the dpp-Bian and 3,6-Cat ligands is 87°.

Compound **5** consists of separated ions, [(dpp-Bian)₂Ag]⁺ (Figure 9) and [BF₄][−]. In the cation dpp-Bians act as neutral chelating ligands. Thus, the C–N distances within both metallacycles in compound **5** (1.260(4), 1.271(4), 1.281(4), 1.276(4) Å) are very close to those bonds in free dpp-Bian (1.282(4) Å)³⁵ as well as in compound (dpp-Bian)SbCl₃,³⁶ which also consists of a neutral dpp-Bian ligand. Due to steric reasons, the dpp-Bians in compound **5** are twisted from each other at 47°. Probably in this geometry the steric repulsion between the isopropyl groups of the dpp-Bian ligands is minimal.

Compound **6** represents a five-coordinate gallium complex (Figure 10). Its coordination polyhedron can be described as a distorted tetragonal pyramid with a basal plane defined by the atoms N(1), N(2), O(1), and O(2). Deviation of the latter from the plane formed with atoms N(1), N(2), and O(1) is

only 0.14 Å. Deviation of the gallium atom from the basal plane toward the axially positioned fluorine ligand is 0.47 Å. The Ga–N distances (2.087(7) and 2.120(1) Å) in **6** are remarkably longer compared to those distances in related compound **4** (1.9432(13) and 1.9335(16) Å), whereas the Ga–O bonds in **4** and **6** (average values: 1.826 and 1.857 Å, correspondingly) are very much alike. Further, the N(1)–C(1) and N(2)–C(2) distances in complex **6** are quite close to those values in compound **5**, which consists of neutral dpp-Bian. The C–O distances in **6** (O(1)–C(37) 1.355(2) and O(2)–C(38) 1.361(2) Å) compare well with those in compound **4** (O(1)–C(37) 1.380(2) and O(2)–C(38) 1.372(2) Å) as well as in catecholates of Ga(III),^{37a} Sn(IV),^{37b–d} and Ge(IV).^{37e} Thus, according to the X-ray data, compound **6** consists of neutral dpp-Bian and dianionic 3,6-di-*tert*-butyl-*ortho*-benzoquinone.

Compound **7** (Figure 11) is situated on the crystallographic 2-fold rotation axis that runs through the centers of the Ga–Ga and C(40)–C(40A) bonds. Reduction of benzylideneacetone with digallane results in radical-anions that recombine to give a 4,5-diphenylocta-2,6-diene-2,7-diolate dianion. In contrast to complex **2**, in which the iodine atoms are *trans*-positioned, the diolate ligand shows a *cis*-coordination to the metallacenter in complex **7**. Due to this chelating effect, the diimine planes are not parallel to each other within a single molecule or between the molecules in the unit cell as in complex **2**. Note, in contrast to compound **2**, complex **7** is well soluble in different organic media, e.g., ethers or aromatic hydrocarbons.

The Ga–Ga bond as well as the Ga–N distances in complex **7** (Ga–Ga, 2.4871(3) Å; Ga–N 2.0075(12) and 2.0258(12) Å) are only slightly longer than corresponding values in compound **2** (Ga–Ga 2.4655(5) Å; Ga–N 1.997(2) and 1.999(2) Å). The newly formed Ga–O bonds (both 1.8456(10) Å) compare well with Ga–O distances in compounds **4** and **6** (average 1.826 and 1.856 Å, correspondingly). The newly formed bond C(40)–C(40A) (1.594(3) Å) is significantly longer than ordinary C–C bonds in alkanes (1.54 Å). However, the C(40)–C(40A) bond in compound **7** is almost the same as a central C–C bond, 1.605(7) Å, in the benzpinacolate ligand formed in the course of recombination of diphenylketyl radicals. The latter were generated from Ph₂C=O under reduction with a magnesium complex of the dpp-Bian dianion (dpp-Bian)Mg(thf)₃.^{12a} The bonds O(1)–C(37), C(39)–C(40), and C(37)–C(39) in compound **7** are altered compared to the free BA.³⁸ The latter bond is shortened to a double bond, while two former bonds became single bonds.

Formation of the C(40)–C(40A) bond makes the carbon atoms involved in the bond formation chiral. It is worth mentioning that in a crystal of compound **7** that was used for the single-crystal X-ray analysis equal quantities of the *R,R* and *S,S* diastereomeric forms were present. A radical-anionic nature of both dpp-Bian ligands in complex **7** is evident from the bond distances within the diimine moiety: the C–N distances are longer than in free dpp-Bian (*vide supra*) but shorter than in the dpp-Bian dianion, for instance in complex **3**.

Organic compound **9** (Figure 12) is a result of the intramolecular addition of the C–H bond of one of the *i*Pr groups to the C=N bond in dpp-Bian. The N(1)–C(1) bond (1.2731(13) Å) is almost the same as the C–N distances in dpp-Bian (1.282(4) Å), while the C(2)–N(2) bond (1.4704(13) Å) corresponds to a single carbon–nitrogen bond. Addition across the C=N bond makes atom C(2) chiral. In the unit cell of compound **9** both enantiomers are present.

Table 1. Crystal Data and Structure Refinement Details for Compounds 2, 3, 4, 5, 6, 7, and 9

	2·C ₄ H ₁₀ O ₂	3·C ₇ H ₈	4·C ₇ H ₈	5·3C ₄ H ₈ O	6	7	9
formula	C ₇₆ H ₉₀ Ga ₂ I ₂ N ₄ O ₂	C ₄₈ H ₅₃ GaIN ₃	C ₅₇ H ₆₈ GaN ₂ O ₂	C ₈₄ H ₁₀₄ AgBF ₄ N ₄ O ₃	C ₅₀ H ₆₀ FGaN ₂ O ₂	C ₁₀₆ H ₁₁₆ Ga ₂ N ₄ O ₂	C ₃₆ H ₄₀ N ₂
M _r [g mol ⁻¹]	1484.76	868.55	882.85	1412.39	809.72	1617.47	500.70
cryst syst	triclinic	monoclinic	monoclinic	monoclinic	orthorhombic	orthorhombic	monoclinic
space group	<i>P</i> $\bar{1}$	<i>P</i> 2 ₁ / <i>n</i>	<i>C</i> 2/ <i>c</i>	<i>P</i> 2 ₁ / <i>c</i>	<i>Pbca</i>	<i>Pnma</i>	<i>P</i> 2 ₁ / <i>c</i>
<i>a</i> [Å]	10.7776(6)	12.2025(4)	26.9451(8)	12.8321(9)	14.9694(10)	24.1618(3)	14.6726(5)
<i>b</i> [Å]	12.9040(7)	19.4990(7)	20.7134(6)	26.0947(17)	19.7485(14)	24.3348(3)	10.2442(3)
<i>c</i> [Å]	14.3443(8)	17.6340(6)	21.8637(6)	23.6182(16)	29.977(2)	14.65391(18)	18.9211(6)
α [deg]	77.3430(10)	90.00	90.00	90.00	90.00	90.00	90.00
β [deg]	70.4290(10)	90.7170(10)	124.4690(10)	105.682(2)	90.00	90.00	92.961(3)
γ [deg]	66.6210(10)	90.00	90.00	90.00	90.00	90.00	90.00
<i>V</i> [Å ³]	1716.76(16)	4195.4(2)	10060.3(5)	7614.2(9)	8862.0(11)	8616.13(18)	2840.20(16)
<i>Z</i>	1	4	8	4	8	4	4
ρ_{calc} [g cm ⁻³]	1.436	1.375	1.166	1.232	1.214	1.247	1.171
μ [mm ⁻¹]	1.732	1.428	0.589	0.325	0.665	0.679	0.067
<i>F</i> (000)	758	1784	3768	2992	3440	3432	1080
crystal size, [mm ³]	0.35 × 0.28 × 0.15	0.15 × 0.10 × 0.08	0.24 × 0.18 × 0.16	0.24 × 0.13 × 0.12	0.23 × 0.20 × 0.03	0.20 × 0.15 × 0.10	0.20 × 0.18 × 0.05
$\theta_{\text{min}}/\theta_{\text{max}}$ [deg]	2.14/26.00	2.04/26.00	2.27/25.00	2.22/26.00	1.84/26.00	2.99/28.00	3.20/25.00
index ranges	-13 ≤ <i>h</i> ≤ 7 -15 ≤ <i>k</i> ≤ 12 -17 ≤ <i>l</i> ≤ 17	-13 ≤ <i>h</i> ≤ 15 -24 ≤ <i>k</i> ≤ 24 -21 ≤ <i>l</i> ≤ 20	-32 ≤ <i>h</i> ≤ 23 -22 ≤ <i>k</i> ≤ 24 -23 ≤ <i>l</i> ≤ 26	-15 ≤ <i>h</i> ≤ 14 -30 ≤ <i>k</i> ≤ 32 -29 ≤ <i>l</i> ≤ 29	-18 ≤ <i>h</i> ≤ 18 -24 ≤ <i>k</i> ≤ 24 -36 ≤ <i>l</i> ≤ 36	-31 ≤ <i>h</i> ≤ 31 -32 ≤ <i>k</i> ≤ 32 -19 ≤ <i>l</i> ≤ 19	-17 ≤ <i>h</i> ≤ 17 -12 ≤ <i>k</i> ≤ 12 -22 ≤ <i>l</i> ≤ 22
reflns collected	10 513	25 227	27 495	45 500	73 311	146 847	38 582
independ reflns	6724	8242	8760	14 876	8699	10 387	4990
<i>R</i> _{int}	0.0299	0.0293	0.0328	0.1121	0.1103	0.1218	0.0402
max/min transmn	0.7812/0.5824	0.8943/0.8144	0.9117/0.8716	0.9621/0.9262	0.9803/0.8621	0.9352/0.8761	0.9966/0.9867
data/ restraints/ params	6724/0/397	8242/0/487	8760/0/574	14 876/80/884	8699/2/536	10 387/128/595	4990/20/407
GOF on <i>F</i> ²	1.023	1.065	1.051	1.000	0.992	1.012	1.043
final <i>R</i> indices [<i>I</i> > 2 σ (<i>I</i>)]	0.0424/0.1091	0.0337/0.0810	0.0487/0.1299	0.0695/0.1369	0.0445/0.0902	0.0418/0.0825	0.0425/0.1050
<i>R</i> indices (all data)	0.0508/0.1143	0.0447/0.0854	0.0654/0.1400	0.1510/0.1569	0.0857/0.1004	0.0737/0.0898	0.0520/0.1097
largest diff peak/hole [e Å ⁻³]	1.860/0.720	1.601/-0.377	1.231/-0.361	1.137/-0.978	0.454/-0.240	0.365/-0.321	0.651/-0.592

CONCLUSION

In an extension of our research we have studied the reactivity of complex (dpp-Bian)Ga–Ga(dpp-Bian) (**1**) toward iodine, 3,6-di-*tert*-butyl-*ortho*-benzoquinone, and benzylideneacetone. In the course of this study a new type of reactivity of compound **1** has been disclosed. We have demonstrated that in the reactions with iodine and benzylideneacetone an oxidation of the dianionic dpp-Bian ligands in complex **1** to radical-anionic state takes place before oxidation of the metal–metal bond. In contrast, the reaction of compound **1** with Me₂N(S)CS–SC(S)NMe₂ proceeds with cleavage of the Ga–Ga bond to give gallium(III) derivative (dpp-Bian)Ga(S₂CNMe₂) (Scheme 1). In this reaction the oxidation state of the ligand is preserved. The dualism of the reactivity of compound **1** is caused by the presence in the molecule of two different redox-active centers. Obviously, the course of reactions of compound **1** is dependent on several factors, mainly the nature of the substrate involved. The bulkiness and coordinative features of the substrate (monodentate, chelating, etc.) are of primary importance. Intuitively, we feel that the ligand-centered oxidation process in

most of the reactions would be preferable compared to the metal-centered oxidation of compound **1**. This supposition may be rationalized in terms of the bulkiness of the dpp-Bian ligand itself. The latter consists of 2,6-*i*Pr₂C₆H₃ groups that may conflict with ligands that coordinate to the metal in the course of the addition reaction. Repulsion between the dpp-Bian and these ligands can be released to some extent when the dpp-Bian ligand is oxidizing from the dianion to the radical-anion. This causes a ca. 0.1 Å elongation of the Ga–N distances.

We believe that the ability of complex **1** to add the substrates in a two-electron oxidative addition manner provides a chance to use complexes like **1** in catalytic reactions of organic synthesis. Another aspect of the chemistry reported here is the redox-isomerism phenomenon in the main-group metal complexes. This phenomenon is well established for transition metal systems. Redox-isomerism is reversible intramolecular metal-to-ligand electron transfer induced thermally or by irradiation. Sometimes metal-to-ligand electron transfer may be induced by solvent. Complex **2** is exactly the latter case. Thus, coordination of pyridine to gallium in complex **2** results in its dissociation to mononuclear species with simultaneous

transfer of an electron from the gallium to the dpp-Bian ligand, resulting in compound **3**. To the best of our knowledge, this is the first observation of such behavior in main-group metal complex. Also complexes **4** and **6** are unique examples, as they consist of two different redox-active ligands. In such systems a redox-isomerism that involves only the ligands can be expected. In the case of compound **6** the two most probable redox-isomers should have the following charge distribution: $(\text{dpp-Bian})^{-}\text{Ga}(\text{F})(3,6\text{-Q})^{-}$ and $(\text{dpp-Bian})^0\text{Ga}(\text{F})(3,6\text{-Q})^{2-}$. The latter has been in fact observed. The stability of the redox-isomers with some degree of probability can be deduced from the reduction potentials of the ligands involved. Thus, the existence of isomer $(\text{dpp-Bian})^{-}\text{Ga}(\text{F})(3,6\text{-Q})^{-}$ of complex **6** cannot be excluded since the first reduction potential of dpp-Bian and the second reduction potential of 3,6-Q are close (both -1.0 V).³⁹ However, in such a situation the redox-isomers as unique species might not exist at all: an electron can be delocalized between two radical-anionic ligands via shuttle transfer from one ligand to another and back, causing no geometrical changes in the molecules, as usually observed in redox-isomers.

In the reaction of compound **1** with BA the formation of a 2+4 cycloadduct may happen. But, one can expect that this cycloadduct is thermodynamically less stable compared to compound **7**, which was isolated, although with only 26% yield. Transformation of the cycloadduct to a more stable product with dpp-Bian radicals has been recently observed in the reaction of $(\text{dpp-Bian})\text{Ga-Ga}(\text{dpp-Bian})$ with $\text{PhC}\equiv\text{CH}$.⁴⁰ Unexpected coupling of the BA radical-anions at the γ position to the oxygen atom is driven probably by the binuclear character of the metal coordination center in compound **1**: with a fixed Ga–Ga bond distance the formation of a C–C bond at the α position would cause tension in the six-membered metallacycle.

EXPERIMENTAL SECTION

General Remarks. All manipulations were carried out under vacuum using glass ampoules. The solvents toluene, diethyl ether, DME, and THF were dried over sodium/benzophenone and pyridine, over sodium. Benzene- d_6 (Aldrich) was dried over sodium/benzophenone at ambient temperature and, just prior to use, condensed under vacuum into the NMR tubes already containing the respective compound. The IR spectra were recorded on a FSM-1201 spectrometer in a Nujol; the ^1H NMR spectra, on a Bruker DPX-200 (200 MHz) and Bruker Avance III (400 MHz) NMR spectrometer. The ESR spectra were obtained using a Bruker EMX spectrometer (9.75 GHz); the signals were referenced to the signal of diphenylpicrylhydrazyl ($g = 2.0037$). The magnetic susceptibilities in the solid state were determined using a SQUID MPMS-XL-5 (Quantum Design) at 5 kOe in the range from 2 to 400 K. The powdered sample was placed in a Teflon bucket and fixed in a nonmagnetic sample holder. Each raw data file for the measured magnetic moment was corrected for the diamagnetic contribution of the sample holder and the Teflon bucket. The molar susceptibility data were corrected for the diamagnetic contribution. Simulation of the experimental magnetic data was performed with the *julX* program (E. Bill, Max-Planck Institute for Chemical Energy Conversion, Mülheim/Ruhr, Germany). Melting points were measured in sealed capillaries. The dpp-Bian was prepared by the condensation of acenaphthene-quinone with 2,6-diisopropylaniline (both from Aldrich) in acetonitrile under reflux. 3,6-Di-*tert*-butyl-*o*-benzoquinone was prepared according to the literature procedure.⁴¹ AgBF_4 was purchased from Aldrich. Starting compound **1** has been prepared by reflux of dpp-Bian (0.5 g, 1.0 mmol) with an excess of gallium metal in toluene (50 mL) and used *in situ* in the reactions described below. The yields of the

products were calculated from the amount of the dpp-Bian used (0.5 g, 1.0 mmol) in the syntheses.

Reaction of Compound 1 with Iodine. Preparation of $(\text{dpp-Bian})\text{Ga-Ga}(\text{dpp-Bian})$ (2**) and $(\text{dpp-Bian})\text{Ga}(\text{Py})$ (**3**).** Addition of iodine (0.13 g, 0.5 mmol) to a deep blue solution of **1** caused an immediate red-brown coloring of the reaction mixture. After removal of the solvent under vacuum 1,2-dimethoxyethane (50 mL) was added to a residual brick-red solid. The ampoule was sealed off under vacuum, and the mixture was heated at 110 °C for 5 h. In 48 h after cooling of the mixture to ambient temperature compound **2** (0.35 g, 47%) was isolated as brown crystals. Mp: >280 °C. IR (Nujol): 1534 vs, 1339 w, 1318 m, 1255 m, 1216 w, 1187 s, 1147 w, 1120 s, 1045 w, 934 m, 895 w, 870 m, 820 s, 802 s, 762 vs, 699 w, 591 w, 549 m, 453 w cm^{-1} . Anal. Calcd for $\text{C}_{72}\text{H}_{80}\text{Ga}_2\text{I}_2\text{N}_4 \times \text{C}_4\text{H}_{10}\text{O}_2$ (1484.76): C, 60.85; H, 5.89. Found: C, 60.48; H, 6.11. In a separate synthesis the crude product **2** left after evaporation of 1,2-dimethoxyethane was dissolved in pyridine (20 mL). All the volatiles were removed from the blue solution, and the residue was crystallized from toluene. Compound **3** was isolated as deep blue crystals (0.55 g, 63%) from toluene. Mp: 253 °C. Anal. Calcd for $\text{C}_{41}\text{H}_{45}\text{GaIN}_3 \times \text{C}_7\text{H}_8$ (868.55): C, 66.25; H, 5.89. Found: C, 66.38; H, 6.15. IR (Nujol): 1601 m, 1589 w, 1512 s, 1461 s, 1435 s, 1358 w, 1331 m, 1317 m, 1260 m, 1213 m, 1180 w, 1136 w, 1106 w, 1068 m, 1044 m, 1017 w, 938 w, 926 m, 902 m, 813 s, 766 vs, 695 s, 645 m, 618 w cm^{-1} . ^1H NMR (400 MHz, C_6D_6): δ 8.61 ppm (d, 2 H, Py, $J = 5.0$ Hz); 7.30–7.26 (m, 4 H, Ar); 7.20–7.15 (m, 2 H, Ar); 7.11 (d, 2 H, Ar, $J = 7.5$ Hz); 7.08 (d, 2 H, Ar, $J = 8.0$ Hz); 7.04 (d, 1 H, Ar); 7.00 (d, 2 H, Py, $J = 7.5$ Hz); 6.90–6.87 (dd, 2 H, Ar, $J_1 = 7.0$ Hz, $J_2 = 7.0$); 6.67–6.60 (pst, 1 H, Py); 6.37 (d, 2 H, Ar, $J = 6.8$ Hz); 6.26–6.21 (pst, 2 H, Ar); 3.95 (sept, 2 H, $\text{CH}(\text{CH}_3)_2$, $J = 6.8$ Hz); 3.27 (sept, 2 H, $\text{CH}(\text{CH}_3)_2$, $J = 6.8$ Hz); 2.1 (s, 3 H, $\text{CH}_3\text{C}_6\text{H}_5$), 1.57 (d, 6 H, $\text{CH}(\text{CH}_3)_2$, $J = 6.8$ Hz); 1.23 (d, 6 H, $\text{CH}(\text{CH}_3)_2$, $J = 6.8$ Hz); 1.13 (d, 6 C, $\text{CH}(\text{CH}_3)_2$, $J = 6.8$ Hz); 0.33 (d, 6 H, $\text{CH}(\text{CH}_3)_2$, $J = 6.8$ Hz).

Reaction of Compound 1 with 3,6-Di-*tert*-butyl-*ortho*-benzoquinone. Synthesis of $(\text{dpp-Bian})\text{Ga}(\text{Cat})$ (4**).** To a solution of **1** in toluene (50 mL) was added 3,6-di-*tert*-butyl-*ortho*-benzoquinone (0.22 g, 1.0 mmol). At 95 °C within 1 h the solution changed color from deep blue to green. Green crystals of complex **4** (80%, 0.71 g) were separated from a concentrated toluene solution. Mp: 265–268 °C. Anal. Calcd for $\text{C}_{57}\text{H}_{68}\text{GaN}_2\text{O}_2$ (882.85): C, 76.64; H, 7.55. Found: C, 77.55; H, 7.76. IR (Nujol): 1593 m, 1536 vs, 1397 s, 1356 w, 1324 m, 1281 w, 1256 s, 1234 vs, 1215 m, 1200 m, 1147 vs, 1114 w, 1082 w, 1060 w, 1041 w, 1025 w, 971 vs, 952 m, 937 m, 920 m, 897 s, 881 m, 836 w, 824 s, 806 s, 793 s, 766 vs, 695 m, 671 w, 649 s, 627 w, 590 w, 550 w, 507 w cm^{-1} . ESR (toluene, 293 K): $a_1(2\ ^{14}\text{N}) = 0.43$, $a_1(^{69}\text{Ga}) = 1.42$, $a_1(^{71}\text{Ga}) = 1.81$, $a_1(2\ ^1\text{H}) = 0.11$, $a_1(2\ ^1\text{H}) = 0.12$ mT, $g = 2.0025$.

Reaction of Compound 4 with AgBF_4 . Formation of $(\text{dpp-Bian})_2\text{Ag}[\text{BF}_4]$ (5**) and $(\text{dpp-Bian})\text{GaF}(\text{Cat})$ (**6**).** To a solution of compound **4** in toluene (50 mL), obtained *in situ* as described above, AgBF_4 (0.19 g, 1.0 mmol) was added. The color of the solution turned from green to brown. Concentration of the solution under vacuum gave orange crystals of compound **5**, which were recrystallized from THF (0.4 g, 57%). Complex **5** was also obtained by the reaction of AgBF_4 (0.1 g, 0.5 mmol) with dpp-Bian (0.5 g, 1 mmol) in THF. Yield: 0.5 g (71%). Mp: 223 °C. Anal. Calcd for $\text{C}_{84}\text{H}_{104}\text{AgBF}_4\text{N}_4\text{O}_3$ (1412.39): C, 72.26; H, 6.81. Found: C, 71.43; H, 7.42. IR (Nujol): 1653 m, 1617 m, 1584 m, 1363 m, 1316 w, 1281 m, 1250 w, 1228 w, 1189 m, 1057 s, 938 w, 836 s, 800 m, 784 m, 759 m, 610 w, 541 m, 521 w cm^{-1} . ^1H NMR of the crude product **5** precipitated from toluene (200 MHz, C_6D_6): δ 7.5–6.5 ppm (m, 24 H, arom.); 3.35 (sept, 8 H, $\text{CH}(\text{CH}_3)_2$, $J = 6.8$ Hz); 1.42 (d, 24 H, $\text{CH}(\text{CH}_3)_2$, $J = 6.8$ Hz); 1.16 (d, 12 H, $\text{CH}(\text{CH}_3)_2$, $J = 6.8$ Hz). Concentration of the toluene solution left after separation of crude **5** gave complex **6** (0.1 g, 25%) as dark green crystals. Mp: 187 °C. Anal. Calcd for $\text{C}_{50}\text{H}_{60}\text{FGaN}_2\text{O}_2$ (809.72): C, 74.17; H, 7.47. Found: C, 73.55; H, 7.76. IR (Nujol): 1665 m, 1630 s, 1583 s, 1411 s, 1366 s, 1326 m, 1294 s, 1254 w, 1226 w, 1208 w, 1182 m, 1134 m, 1090 s, 1056 s, 970 m, 955 s, 850 m, 838 s, 806 s, 797 m, 782 s, 764 m, 757 m, 731 m, 695 m, 681 s, 654 s, 617 w, 583 m, 546 m, 516 w, 502 m, 405 w cm^{-1} . ^1H

NMR (200 MHz, CDCl₃): δ 8.20 ppm (d, 2 H, Ar, $J = 8.3$ Hz); 7.66 (t, 2 H, Ar, $J = 7.5$ Hz); 7.51 (s, 2 H, CH Cat); 7.07 (d, 2 H, Ar, $J = 7.3$ Hz); 3.66 (sept, 2 H, CH(CH₃)₂, $J = 6.8$ Hz); 2.64 (sept, 2 H, CH(CH₃)₂, $J = 6.8$ Hz); 1.47 (d, 6 H, CH(CH₃)₂, $J = 6.8$ Hz), 1.18 (d, 6 H, CH(CH₃)₂, $J = 6.8$ Hz); 1.05 (m, 24 H, C(CH₃)₃, CH(CH₃)₂), 0.69 (d, 6 H, CH(CH₃)₂, $J = 6.8$ Hz).

Reaction of Compound 1 with Benzylideneacetone. Formation of (dpp-Bian)Ga(BA–BA)–Ga(dpp-Bian) (7), (dpp-Bian)Ga(BA–BA) (8), and C₃₆H₄₀N₂ (9). To a solution of **1** in toluene (50 mL) was added benzylideneacetone (0.15 g, 1.0 mmol). Within 10 min at ambient temperature the color of solution turned brown. Concentration of the toluene solution under vacuum caused the precipitation of dark brown crystals of complex **7** (0.41 g, 26%). Mp: 143 °C. Anal. Calcd for C₁₀₆H₁₁₆Ga₂N₄O₂ (1617.47): C, 78.71; H, 7.23. Found: C, 78.28; H, 7.18. IR (Nujol): 1645 m, 1598 w, 1537 s, 1479 m, 1362 m, 1317 m, 1267 m, 1193 m, 1186 m, 1144 w, 1112 w, 1080 w, 1040 w, 1013 w, 945 w, 934 w, 888 w, 866 w, 854 w, 842 w, 821 m, 802 m, 771 m, 761 m, 752 w, 700 m, 671 w, 638 w, 619 w, 595 w, 545 w, 515 w, 457 w cm⁻¹. ESR (toluene, 150 K): |D| = 10.0 mT, |E| = 0.8 mT. In a separate experiment the initial reaction mixture formed after treatment of **1** with benzylideneacetone was heated for 10 min at 95 °C. The heating of the reaction mixture caused the appearance of the ESR signal ($a_{\text{N}}(2 \times ^{14}\text{N}) = 0.48$ mT, $a_{\text{Ga}}(^{69}\text{Ga}) = 1.13$ mT, $a_{\text{Ga}}(^{71}\text{Ga}) = 1.43$ mT, $g_{\text{N}} = 2.0026$), which indicates the formation of compound (dpp-Bian)Ga(BA–BA) (**8**). Evaporation of the solvent and crystallization of the residual solid from diethyl ether resulted in compound **9** (0.21 g, 40%). Mp: 163–167 °C. Anal. Calcd for C₃₆H₄₀N₂ (500.70): C, 86.35; H, 8.05. Found: C, 85.58; H 7.95. IR (Nujol): 1656 s, 1620 w, 1598 m, 1435 s, 1377 s, 1325 m, 1250 m, 1184 w, 1162 w, 1112 w, 1068 m, 1023 m, 955 w, 935 w, 919 w, 902 m, 830 m, 786 s, 753 s, 679 w, 610 m, 516 m cm⁻¹. ¹H NMR (400 MHz, C₆D₆): δ 7.59 (d, 1 H, Ar, $J = 6.9$ Hz), 7.42 (pst, 2 H, Ar, $J = 7.4$ Hz), 7.28 (d, 1 H, Ar, $J = 7.1$ Hz), 7.24–6.93 (m, 6 H, Ar), 6.86 (pst, 1 H, Ar, $J = 7.1$ Hz), 6.74 (m, 1H, Ar, $J = 7.1$ Hz), 4.71 (s, 1 H, NH), 3.22, 3.01, 2.58 (all sept, 3 × 1 H, CH(CH₃)₂, $J = 6.8$ Hz), 1.41 (s, 3 H, C(CH₃)₂), 1.32 (d, 3 H, CH(CH₃)₂, $J = 6.8$ Hz), 1.29–1.20 (m, 9 H, CH(CH₃)₂, C(CH₃)₂), 1.10–0.96 (dd, 6 H, CH(CH₃)₂, $J = 6.8$ Hz, $J = 7.0$ Hz), 0.52 (d, 3 H, CH(CH₃)₂, $J = 7.0$ Hz). Unfortunately, we were not able to isolate compound **8** in the solid state.

Single-Crystal X-ray Structure Determination of 2–7 and 9. The X-ray data for **2–6** were collected on a Smart Apex diffractometer (graphite-monochromated Mo K α radiation, ω -scan technique, $\lambda = 0.71073$ Å) at $T = 100(2)$ K for **3–6** and $150(2)$ K for **2**. The data for **7** and **9** were obtained on an Agilent Xcalibur E diffractometer (graphite-monochromated Mo K α radiation, ω -scan technique, $\lambda = 0.71073$ Å) at $T = 100(2)$ K. The structures were solved by direct methods and were refined on F^2 using SHELXTL⁴² (**2–6**) and the CrysAlis Pro⁴³ package (**7** and **9**). All hydrogen atoms were placed in calculated positions and were refined in the riding mode. SADABS⁴⁴ (**2–6**) and ABSPACK (CrysAlis Pro)⁴³ (**7** and **9**) were used to perform area-detector scaling and absorption corrections. Experimental details are given in Table 1.

■ ASSOCIATED CONTENT

Ⓢ Supporting Information

This material is available free of charge via the Internet at <http://pubs.acs.org>.

■ AUTHOR INFORMATION

Corresponding Author

*E-mail: igorfed@iomc.ras.ru.

Notes

The authors declare no competing financial interest.

■ ACKNOWLEDGMENTS

This work was supported by the Russian Science Foundation (grant 14-13-01063).

■ DEDICATION

Dedicated to Professor Mikhail N. Bochkarev on the occasion of his 75th birthday.

■ REFERENCES

- (1) (a) Grützmacher, H. *Angew. Chem., Int. Ed.* **2008**, *47*, 1814–1818. (b) Kaim, W.; Schwederski, B. *Coord. Chem. Rev.* **2010**, *254*, 1580–1588. (c) Dzik, W. I.; van der Vlugt, J. I.; Reek, J. N. H.; de Bruin, B. *Angew. Chem., Int. Ed.* **2011**, *50*, 3356–3358. (d) van der Vlugt, J. I. *Eur. J. Inorg. Chem.* **2012**, *3*, 363–375. (e) Lyaskovskyy, V.; de Bruin, B. *ACS Catal.* **2012**, *2*, 270–279. (f) Chirik, P. J. *Inorg. Chem.* **2011**, *50*, 9737–9740.
- (2) (a) Lyons, T. W.; Sanford, M. S. *Chem. Rev.* **2010**, *110*, 1147–1169. (b) Mkhaldid, I. A. I.; Barnard, J. H.; Marder, T. B.; Murphy, J. M.; Hartwig, J. F. *Chem. Rev.* **2010**, *110*, 890–931. (c) Wu, X.-F.; Neumann, H.; Beller, M. *Chem. Rev.* **2013**, *113*, 1–35. (d) Zeng, X. *Chem. Rev.* **2013**, *113*, 6864–6900. (e) Beletskaya, I. P.; Cheprakov, A. V. *Chem. Rev.* **2000**, *100*, 3009–3066. (f) Colby, D. A.; Bergman, R. G.; Ellman, J. A. *Chem. Rev.* **2010**, *110*, 624–655. (g) Bellina, F.; Rossi, R. *Chem. Rev.* **2010**, *110*, 1082–1146. (h) Beletskaya, I. P.; Ananikov, V. P. *Chem. Rev.* **2011**, *111*, 1596–1636. (i) Climent, M. J.; Corma, A.; Iborra, S. *Chem. Rev.* **2011**, *111*, 1072–1133. (j) Carsten, B.; He, F.; Son, H. J.; Xu, T.; Yu, L. *Chem. Rev.* **2011**, *111*, 1493–1528. (k) Jana, R.; Pathak, T. P.; Sigman, M. S. *Chem. Rev.* **2011**, *111*, 1417–1492. (l) Molnár, Á. *Chem. Rev.* **2011**, *111*, 2251–2320.
- (3) (a) Königsmann, M.; Donati, N.; Stein, D.; Schönberg, H.; Harmer, J.; Sreekanth, A.; Grützmacher, H. *Angew. Chem., Int. Ed.* **2007**, *46*, 3567–3570. (b) Ringenberg, M. R.; Kokatam, S. L.; Heiden, Z. M.; Rauchfuss, T. B. *J. Am. Chem. Soc.* **2008**, *130*, 788–789. (c) Ringenberg, M. R.; Rauchfuss, T. B. *Eur. J. Inorg. Chem.* **2012**, *3*, 490–495.
- (4) Lorkovic, I. M.; Duff, R. R., Jr.; Wrighton, M. S. *J. Am. Chem. Soc.* **1995**, *117*, 3617–3618.
- (5) (a) Bouwkamp, M. W.; Bowman, A. C.; Lobkovsky, E.; Chirik, P. J. *J. Am. Chem. Soc.* **2006**, *128*, 13340–13341. (b) Chirik, P. J.; Wieghardt, K. *Science* **2010**, *327*, 794–795.
- (6) (a) Lippert, C. A.; Arnstein, S. A.; Sherrill, C. D.; Soper, J. D. *J. Am. Chem. Soc.* **2010**, *132*, 3879–3892. (b) Lippert, C. A.; Riener, K.; Soper, J. D. *Eur. J. Inorg. Chem.* **2012**, *3*, 554–561.
- (7) (a) Blackmore, K. J.; Lal, N.; Ziller, J. W.; Heyduk, A. F. *J. Am. Chem. Soc.* **2008**, *130*, 2728–2729. (b) Heyduk, A. F.; Zarkesh, R. A.; Nguyen, A. I. *Inorg. Chem.* **2011**, *50*, 9849–9863.
- (8) (a) de Bruin, T. J. M.; Magna, L.; Raybaud, P.; Toulhoat, H. *Organometallics* **2003**, *22*, 3404–3413. (b) Blok, A. N. J.; Budzelaar, P. H. M.; Gal, A. W. *Organometallics* **2003**, *22*, 2564–2570. (c) Otten, E.; Batinas, A. A.; Meetsma, A.; Hessen, B. *J. Am. Chem. Soc.* **2009**, *131*, 5298–5312. (d) Tsurugi, H.; Saito, T.; Tanahashi, H.; Arnold, J.; Mashima, K. *J. Am. Chem. Soc.* **2011**, *133*, 18673–18683.
- (9) Otten, E.; Meetsma, A.; Hessen, B. *J. Am. Chem. Soc.* **2007**, *129*, 10100–10101.
- (10) (a) Chaudhuri, P.; Hess, M.; Flörke, U.; Wieghardt, K. *Angew. Chem., Int. Ed.* **1998**, *37*, 2217–2220. (b) Whittaker, J. W. *Chem. Rev.* **2003**, *103*, 2347–2363. (c) Que, L.; Tolman, W. B. *Nature* **2008**, *455*, 333–340.
- (11) Fedushkin, I. L.; Skatova, A. A.; Chudakova, V. A.; Fukin, G. K.; Dechert, S.; Schumann, H. *Eur. J. Inorg. Chem.* **2003**, 3336–3346.
- (12) (a) Fedushkin, I. L.; Skatova, A. A.; Cherkasov, V. K.; Chudakova, V. A.; Dechert, S.; Hummert, M.; Schumann, H. *Eur. J.* **2003**, *9*, 5778–5783. (b) Fedushkin, I. L.; Khvoynova, N. M.; Skatova, A. A.; Fukin, G. K. *Angew. Chem.* **2003**, *115*, 5381–5384; *Angew. Chem., Int. Ed.* **2003**, *42*, 5223–5226. (c) Fedushkin, I. L.; Chudakova, V. A.; Fukin, G. K.; Dechert, S.; Hummert, M.; Schumann, H. *Russ. Chem. Bull.* **2004**, *53*, 2744–2750. (d) Fedushkin, I. L.; Skatova, A. A.; Fukin, G. K.; Hummert, M.; Schumann, H. *Eur. J. Inorg. Chem.* **2005**, 2332–2338. (e) Fedushkin, I. L.; Skatova, A. A.; Lukoyanov, A. N.; Chudakova, V. A.; Dechert, S.; Hummert, M.; Schumann, H. *Russ. Chem. Bull.* **2004**, *53*, 2751–2762. (f) Fedushkin, I. L.; Morozov, A. G.; Rassadin, O. V.; Fukin, G. K. *Chem.—Eur. J.*

2005, 11, 5749–5757. (g) Fedushkin, I. L.; Makarov, V. M.; Rosenthal, E. C. E.; Fukin, G. K. *Eur. J. Inorg. Chem.* **2006**, 827–832.

(13) The only examples of transition metal compounds containing anionic dpp-Bian ligands are chromium complexes (dpp-Bian)_{Cr}(μ-Cl)₃Mg(thf)₃, [(dpp-Bian)Cr(μ-Cl)(thf)]₂, and [(dpp-Bian)₂Cr][Na(thf)₆]: (a) Fedushkin, I. L.; Makarov, V. M.; Sokolov, V. G.; Fukin, G. K. *Dalton Trans.* **2009**, 8047–8053. For transition metal complexes of the neutral dpp-Bian ligand see: (b) van Laren, M. W.; Elsevier, C. J. *Angew. Chem.* **1999**, 111, 3926–3929; *Angew. Chem., Int. Ed.* **1999**, 38, 3715–3717. (c) van Belzen, R.; Hoffmann, H.; Elsevier, C. J. *Angew. Chem.* **1997**, 109, 1833–1835; *Angew. Chem., Int. Ed. Engl.* **1997**, 36, 1743–1745. (d) Grasa, G. A.; Singh, R.; Stevens, E. D.; Nolan, S. P. *J. Organomet. Chem.* **2003**, 687, 269–279. (e) Heumann, A.; Giordano, L.; Tenaglia, A. *Tetrahedron Lett.* **2003**, 44, 1515–1518. (f) Cherian, A. E.; Lobkovsky, E. B.; Coates, G. W. *Chem. Commun.* **2003**, 2566–2567. (g) Leatherman, M. D.; Svejda, S. A.; Johnson, L. K.; Brookhart, M. J. *Am. Chem. Soc.* **2003**, 125, 3068–3081. (h) Kiesewetter, J.; Kaminsky, W. *Chem.—Eur. J.* **2003**, 9, 1750–1758. (i) Coventry, D. N.; Batsanov, A. S.; Goeta, A. E.; Howard, J. A.; Marder, T. B. *Polyhedron* **2004**, 23, 2789–2795. (j) El-Ayaan, U. *Monatsh. Chem.* **2004**, 135, 919–925. (k) Fedushkin, I. L.; Skatova, A. A.; Lukoyanov, A. N.; Khvoynova, N. M.; Piskunov, A. V.; Nikipelov, A. S.; Fukin, G. K.; Lysenko, K. A.; Irran, E.; Schumann, H. *Dalton Trans.* **2009**, 4689–4694. (l) Fedushkin, I. L.; Eremenko, O. V.; Skatova, A. A.; Piskunov, A. V.; Fukin, G. K.; Ketkov, S. Yu.; Irran, E.; Schumann, G. *Organometallics* **2009**, 28, 3863–3868. (m) Sgro, M. J.; Stephan, D. W. *Dalton Trans.* **2010**, 39, 5786–5794. (n) Kern, T.; Monkowius, U.; Zabel, M.; Knör, G. *Inorg. Chim. Acta* **2011**, 374, 632–636.

(14) (a) Fedushkin, I. L.; Skatova, A. A.; Chudakova, V. A.; Fukin, G. K. *Angew. Chem.* **2003**, 115, 3416–3420; *Angew. Chem., Int. Ed.* **2003**, 42, 3294–3298. (b) Fedushkin, I. L.; Skatova, A. A.; Chudakova, V. A.; Cherkasov, V. K.; Fukin, G. K.; Lopatin, M. A. *Eur. J. Inorg. Chem.* **2004**, 388–393. (c) Fedushkin, I. L.; Chudakova, V. A.; Skatova, A. A.; Khvoynova, N. M.; Kurskii, Yu. A.; Glukhova, T. A.; Fukin, G. K.; Dechert, S.; Hummert, M.; Schumann, H. *Z. Anorg. Allg. Chem.* **2004**, 630, 501–507. (d) Fedushkin, I. L.; Khvoynova, N. M.; Baurin, A. Yu.; Fukin, G. K.; Cherkasov, V. K.; Bubnov, M. P. *Inorg. Chem.* **2004**, 43, 7807–7815. (e) Fedushkin, I. L.; Skatova, A. A.; Chudakova, V. A.; Khvoynova, N. M.; Baurin, A. Yu.; Dechert, S.; Hummert, M.; Schumann, H. *Organometallics* **2004**, 23, 3714–3718. (f) Fedushkin, I. L.; Skatova, A. A.; Chudakova, V. A.; Cherkasov, V. K.; Dechert, S.; Schumann, H. *Russ. Chem. Bull.* **2004**, 53, 2142–2147. (g) Schumann, H.; Hummert, M.; Lukoyanov, A. N.; Fedushkin, I. L. *Organometallics* **2005**, 24, 3891–3896.

(15) Hill, N. J.; Vargas-Baca, I.; Cowley, A. H. *Dalton Trans.* **2009**, 240–253.

(16) Fedushkin, I. L.; Maslova, O. V.; Hummert, M.; Schumann, H. *Inorg. Chem.* **2010**, 49, 2901–2910.

(17) Fedushkin, I. L.; Lukoyanov, A. N.; Tishkina, A. N.; Fukin, G. K.; Lyssenko, K. A.; Hummert, M. *Chem.—Eur. J.* **2010**, 16 (25), 7563–7571.

(18) Fedushkin, I. L.; Nikipelov, A. S.; Skatova, A. A.; Maslova, O. V.; Lukoyanov, A. N.; Fukin, G. K.; Cherkasov, A. V. *Eur. J. Inorg. Chem.* **2009**, 3742–3749.

(19) (a) Fedushkin, I. L.; Nikipelov, A. S.; Lyssenko, K. A. *J. Am. Chem. Soc.* **2010**, 132, 7874–7875. (b) Fedushkin, I. L.; Nikipelov, A. S.; Morozov, A. G.; Skatova, A. A.; Cherkasov, A. V.; Abakumov, G. A. *Chem.—Eur. J.* **2012**, 18, 255–266.

(20) (a) Dabb, S. L.; Messerle, B. A. *Dalton Trans.* **2008**, 6368–6371. (b) Shaffer, A. R.; Schmidt, J. A. R. *Organometallics* **2008**, 27, 1259–1266. (c) Shi, Y.; Ciszewski, J. T.; Odom, A. L. *Organometallics* **2002**, 21, 5148.

(21) Uhl, W.; Layh, M. Formal Oxidation State +2: Metal–Metal Bonded Versus Mononuclear Derivatives. In *The Group 13 Metals Aluminium, Gallium, Indium and Thallium: Chemical Patterns and Peculiarities*; Simon, A., Anthony, J. D., Eds.; John Wiley & Sons: New York, 2011; pp 246–284.

(22) Baker, R. J.; Jones, C.; Kloth, M.; Mills, D. P. *New J. Chem.* **2004**, 28, 207–213.

(23) Tezgerevska, T.; Alley, K. G.; Boskovic, C. *Coord. Chem. Rev.* **2014**, DOI: 10.1016/j.ccr.2014.01.014.

(24) (a) Fedushkin, I. L.; Maslova, O. V.; Morozov, A. G.; Dechert, S.; Demeshko, S.; Meyer, F. *Angew. Chem., Int. Ed.* **2012**, 51, 10584–10587. (b) Fedushkin, I. L.; Maslova, O. V.; Baranov, E. V.; Shavyrin, A. S. *Inorg. Chem.* **2009**, 48, 2355–2357.

(25) Tuononen, H. M.; Armstrong, A. F. *Dalton Trans.* **2006**, 1885–1894.

(26) Allan, C. J.; Cooper, B. F. T.; Cowley, H. J.; Rawson, J. M.; Macdonald, C. L. B. *Chem.—Eur. J.* **2013**, 19, 14470–14483.

(27) Emsley, J. *The Elements*; Clarendon Press: Oxford, 1991.

(28) Piskunov, A. V.; Maleeva, A. I.; Fukin, G. K.; Baranov, E. V.; Bogomyakov, A. S.; Cherkasov, V. K.; Abakumov, G. A. *Dalton Trans.* **2011**, 40, 718–725.

(29) Fedushkin, I. L.; Moskalev, M. V.; Baranov, E. V.; Abakumov, G. A. *J. Organomet. Chem.* **2013**, 747, 235–240.

(30) Fedushkin, I. L.; Lukoyanov, A. N.; Ketkov, S. Y.; Hummert, M.; Schumann, H. *Chem.—Eur. J.* **2007**, 13, 7050–7056.

(31) (a) Baker, R. J.; Farley, R. D.; Jones, C.; Kloth, M.; Murphy, D. M. *Dalton Trans.* **2002**, 3844–3850. (b) Baker, R. J.; Farley, R. D.; Jones, C.; Mills, D. P.; Kloth, M.; Murphy, D. M. *Chem.—Eur. J.* **2005**, 11, 2972–2982.

(32) Delhaes, P. *Graphite and Precursors*; CRC Press: Boca Raton, FL, 2001.

(33) Fedushkin, I. L.; Petrovskaya, T. V.; Girgsdies, F.; Nevodchikov, V. I.; Weimann, R.; Schumann, H.; Bochkarev, M. N. *Russ. Chem. Bull. Int. Ed.* **2000**, 49, 1869–1876.

(34) Fukin, G. K.; Cherkasov, A. V.; Shurygina, M. P.; Druzhkov, N. O.; Kuropatov, V. A.; Chesnokov, S. A.; Abakumov, G. A. *Struct. Chem.* **2010**, 21, 607–611.

(35) Fedushkin, I. L.; Chudakova, V. A.; Fukin, G. K.; Dechert, S.; Hummert, M.; Schumann, H. *Russ. Chem. Bull. Int. Ed.* **2004**, 53, 2744–2750.

(36) Fedushkin, I. L.; Khvoynova, N. M.; Baurin, A. Yu.; Chudakova, V. A.; Skatova, A. A.; Cherkasov, V. K.; Fukin, G. K.; Baranov, E. V. *Russ. Chem. Bull. Int. Ed.* **2006**, 55, 74–83.

(37) (a) Piskunov, A. V.; Mescheryakova, I. N.; Maleeva, A. V.; Fukin, G. K. *Eur. J. Inorg. Chem.* **2012**, 4318–4326. (b) Agustín, D.; Rima, G.; Gornitzka, H.; Barrau, J. *J. Organomet. Chem.* **1999**, 592, 1–10. (c) Lado, A. V.; Poddel'sky, A. I.; Piskunov, A. V.; Fukin, G. K.; Ikorskii, V. N.; Cherkasov, V. K.; Abakumov, G. A. *Inorg. Chim. Acta* **2005**, 358, 4443–4450. (d) Piskunov, A. V.; Lado, A. V.; Fukin, G. K.; Baranov, E. V.; Abakumova, L. G.; Cherkasov, V. K.; Abakumov, G. A. *Heteroat. Chem.* **2006**, 17, 481–490. (e) Lado, A. V.; Piskunov, A. V.; Zhdanovich, I. V.; Fukin, G. K.; Baranov, E. V. *Russ. J. Coord. Chem. (Engl. Transl.)* **2008**, 34, 251–255.

(38) Degen, A.; Bolte, M. *Acta Crystallogr. Sect. C: Cryst. Struct. Commun.* **1999**, 55, IUC9900170.

(39) (a) The reduction potential of dpp-Bian has been estimated using quantum chemical calculations: Baranovski, V. I.; Denisova, A. S.; Kuklo, L. I. *THEOCHEM* **2006**, 759, 111–115. (b) Measured in THF–acetonitrile (4:1) relative to the Ag/AgCl electrode: Letichevskaya, N. N.; Shinkar, E. V.; Berberova, N. T.; Okhlobystin, O. Y. *Russ. J. Gen. Chem.* **1996**, 66, 1785–1787.

(40) Fedushkin, I. L.; Moskalev, M. V.; Lukoyanov, A. N.; Tishkina, A. N.; Baranov, E. V.; Abakumov, G. A. *Chem.—Eur. J.* **2012**, 18, 11264–11276.

(41) Garnov, V. A.; Nevodchikov, V. I.; Abakumova, L. G.; Abakumov, G. A.; Cherkasov, V. K. *Russ. Chem. Bull.* **1987**, 36, 1728–1730.

(42) Sheldrick, G. M. *SHELXTL v.6.12*, Structure Determination Software Suite; Bruker AXS: Madison, WI, USA, 2000.

(43) Agilent Technologies. *CrysAlis Pro*; Agilent Technologies Ltd: Yarnton, England, 2011.

(44) Sheldrick, G. M. *SADABS v.2.01*, Bruker/Siemens Area Detector Absorption Correction Program; Bruker AXS: Madison, WI, USA, 1998.